Integration of Carbon Nanotubes in Silicon Strip and Slot Waveguide Micro-Ring Resonators

Elena Durán-Valdeiglesias, Weiwei Zhang, Adrien Noury, Carlos Alonso-Ramos, Thi Hong Cam Hoang, Samuel Serna, Xavier Le Roux, Eric Cassan, Nicolas Izard, Francesco Sarti, Ughetta Torrini, Francesco Biccari, Anna Vinattieri, Matteo Balestrieri, Al-Saleh Keita, Hongliu Yang, Viktor Bezugly, Gianaurelio Cuniberti, Arianna Filoramo, Massimo Gurioli, and Laurent Vivien

***Abstract*—Silicon photonics has emerged as a very promising technology platform for the implementation of high-performance, low-cost, ultra-compact circuits that can monolithically co-integrate electronic, opto-electronic and optic functionalities. However, Si neither has efficient light emission or detection in the telecom wavelength range, nor exhibits efficient electro-optic Pockels effect, hindering the implementation of integrated active devices like sources, detectors, or modulators. Current approaches relay on different materials to provide active functionalities in Si photonics, resulting in highly complex integration schemes that compromise cost-effectiveness. Semiconducting single-wall carbon nanotubes (SWNTs) are capable of emitting and detecting near-infrared light at room temperature and exhibit intrinsically fast electro-optic effects. They have also proven promising uses in micro-electronic devices, making them an ideal material to provide active functionalities in the Si photonic platform. In this work, we propose and experimentally validate the possible use of slot photonic waveguides to improve interaction between SWNTs and Si waveguide modes. Fabricated Si slot micro-ring shown an experimental $\sim 60\%$ photo-luminescence improvement compared to previous demonstration based on Si strip waveguide resonators. These results prove the potential of Si slot waveguides for the implementation of efficient SWNT-based Si photonic devices.**

***Index Terms*—Carbon nanotubes, light emission, ring resonator, silicon photonics.**

Manuscript received October 22, 2015; revised February 18, 2016; accepted April 05, 2016. Date of publication April 21, 2016; date of current version July 07, 2016. The work of W. Zang, S. Serna, and A. Noury was supported by the Ministry of Higher Education and Research (France). The work of T. H. C. Hoang was supported by the Ministry of Education and Training (Vietnam). This work was supported in parts by the European project FET CARTOON, and by the ANR JCJC project "Ca (Re-) Lase !", and by the French Renatech network. The fabrication of the device was performed at the nano-center CTU-IEF-Minerve, which was supported in part by the 'Conseil Général de l'Essonne'.

E. Durán-Valdeiglesias, W. Zhang, C. Alonso-Ramos, T. H. C. Hoang, X. Le Roux, E. Cassan, N. Izard, and L. Vivien are with the Institute of Electric Fondamentale, University of Paris Sud, CNRS UMR 8622, Université Paris-Saclay, Orsay F-91405, France (e-mail: elena.duran@u-psud.fr; weiwei.zhang1@u-psud.fr; carlos.ramos@u-psud.fr; thi-hong-cam.hoang@u-psud.fr; xavier.leroux@u-psud.fr; eric.cassan@u-psud.fr; nicolas.izard@univ-montp2.fr; laurent.vivien@u-psud.fr).

S. Serna is the Institute of Electric Fondamentale, University of Paris Sud, CNRS UMR 8622, Université Paris-Saclay, Orsay F-91405, France and the Laboratoire of Charles Fabry, Institut d'Optique Graduate School, CNRS, Université Paris Saclay, Palaiseau Cedex 91127, France (e-mail: samuel.serna@u-psud.fr).

F. Sarti, U. Torrini, F. Biccari, A. Vinattieri, and M. Gurioli are with the Department of Physics, University of Florence, European Laboratory for Nonlinear Spectroscopy, Sesto Fiorentino 50019, Italy (e-mail: sarti@lens.unifi.it; ughettatorrini@gmail.com; francesco.biccari@unifi.it; vinattieri@fi.infn.it; gurioli@lens.unifi.it).

H. Yang, V. Bezugly, and G. Cuniberti are with the Technische Universitaet Dresden, Institute for Materials Science, Dresden 01062, Germany (e-mail: hyang@nano.tu-dresden.de; viktor.bezugly@nano.tu-dresden.de; g.cuniberti@tu-dresden.de).

M. Balestrieri, A.-S. Keita, and A. Filoramo are with CEA Saclay, IRAMIS, NIMBE (UMR 3685), LICSEN, F-91191Gif-sur-Yvette, France (e-mail: matteo.balestrieri@cea.fr; al-saleh.keita@cea.fr; arianna.filoramo@cea.fr).

A. Noury is with the ICFO-Intitut de CienciesFotoniques, Mediterranean Technology Park, Castelldefels 08860, Barcelona, Spain (e-mail: adrien.noury@icfo.es).

Color versions of one or more of the figures in this paper are available online at http://ieeexplore.ieee.org.

Digital Object Identifier 10.1109/TNANO.2016.2556225

I. Introduction

BANDWIDTH-HUNGRY applications such as video streaming, social networking, or web search relay on a large network of data centres, interconnected through optical links [1]. The ever-growing data rates and power consumption inside these data centres are pushing copper links close to their fundamental limits. Hence, photonic interconnects are being extensively developed, aiming to overcome these limitations, to replace electrical interconnects in the short link communications [2]. For instance, active optoelectronic cables are successfully commercialized by the company Luxtera since 2006 [3]. Besides, the increasing gap between the computational capacity and electrical bandwidth in high-performance computing systems is also driving the development of rack-to-rack and even chip-to-chip photonic links [4]. On the other hand, and motivated by the successful development in the telecommunications field, photonics is also being considered for other applications such as biosensing [5] or hazard detection [6]. In this context, silicon photonics has emerged as a very promising technology platform that enables the implementation of ultra-compact and high-performance devices [7]. Furthermore, due to its compatibility with the Si processes, silicon photonics has the unique potential to deliver devices that can co-integrate electronic, opto-electronic and photonic functionalities within a single chip that can be produced at a very large volume and very low cost. This features made companies such as IBM [8], Intel [9] and Oracle [10] choose silicon, and specifically silicon-on-insulator (SOI) as the preferred platform for the development of their photonic interconnects. However, silicon presents some fundamental limitations as a material for photonic technologies. Silicon is an indirect gap semiconductor, resulting in non-efficient light emission, and its transparency in telecommunication wavelength range $(1.3\ \mu\mathrm{m} - 1.5\ \mu\mathrm{m})$ avoids efficient detection. Hence, silicon photonics needs to be complemented with other materials for the implementation of active devices, including Ge for detectors and III-V semiconductors for laser sources [11]–[13]. In addition, the centro-symmetry of Si crystalline structure

inhibits linear electro-optic modulation of light based on Pockels effect. To overcome this limitation state-of-the-art Si modulators rely on the plasma dispersion effects in highly doped Si waveguides. This approach results in added propagation loss and power consumption. Due to the various materials used, the integration of all these photonic and optoelectronic building blocks in the same chip is very complex and is not cost-effective. Indeed, the integration of a broad variety of materials on the Si platform leads to a very complex heterogeneous integration scheme, offsetting the low-cost provided by the use of Si. Furthermore, III-V technology is not fully compatible with Si technology and new sophisticated processes have yet to be developed for effective integration.

Carbon nanotubes (CNTs), due to their very good chemical stability, electrical conductivity and Si compatibility, have been identified as a very promising material for future Si microelectronics [14]. For instance, they have been widely investigated for the implementation of CNT-based Si field effect transistors [15]. However, it has not been until very recently that CNTs have also been considered as a very attractive material for future Si photonics. Interestingly, semiconducting single wall CNTs (SWNTs) exhibit room-temperature photo- and electroluminescence in the near-IR that could be exploited for the implementation of integrated sources [16]. They also can be considered for the realization of photo-detectors and optical modulators relying on intrinsically fast non-linear (Stark and Kerr) effects [17], [18]. These properties make SWNTs ideal candidates to realize all the main optoelectronic devices, including near-IR sources, modulators and photodetectors in the Si photonic platform.

Pioneering works have already demonstrated coupling of light emission from SWNTs into silicon waveguides [16], [19] and intrinsic room-temperature optical gain at 1.3 μm wavelength [20]. These milestones opened the door to the implementation of an integrated laser on Si employing SWNTs as gain medium. Nevertheless, two major challenges need to be addressed to enable the realization of such device: improve the coupling of SWNTs emitted light into Si waveguides and overcome the SWNTs low quantum efficiency. Various strategies have been proposed to alleviate SWNTs low quantum efficiency, based on the use of Si photonic microcavities [21]–[25]. However, very little attention has been devoted to develop Si photonic waveguides that maximize interaction with SWNTs. Indeed, only strip waveguides have been considered for integration of SWNTs in Si photonic devices [26].

In this work, we study theoretically and experimentally the interaction of two different Si photonic waveguides, strip and slot, with SWNTs. We experimentally prove the improved behavior of SWNTs-filled Si slot waveguides, compared with previously used Si strip waveguides' configurations. To carry out this work, we have compared photoluminescence (PL) enhancement in micro-ring resonators implemented using Si strip and slot waveguides, showing that slot micro-rings exhibit a superior performance.

This paper is organized as follows. In Section II we analyze the modal properties of the proposed, Si strip and slot, waveguides. Experimental characterization of SWNT photoluminescence enhancement in strip and slot micro-ring resonators is described in Section III. Finally, Section IV summarizes the main conclusions of this work.

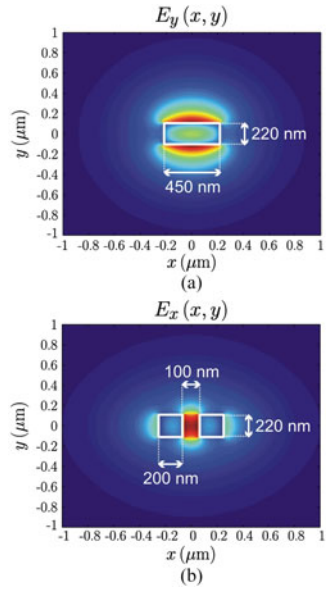

Fig. 1. Electric field distribution at 1300 nm wavelength for: (a) TM mode (Electric field E_y) of strip waveguide and (b) TE mode (Electric field E_x) of slot waveguide.

II. Analysis of Silicon Photonic Waveguides

To favor the interaction with SWNTs, it is desirable to have photonic waveguides that maximize the overlap between optical mode field and the surrounding media (where the SWNTs are deposited or dispersed) and simultaneously minimize the propagation losses. In this work we have considered Si strip and slot waveguides exhibiting high interaction with the surrounding medium (Fig. 1) and low propagation loss [5].

We have analyzed the modal properties of two silicon-on-insulator photonic integrated waveguide configurations: strip waveguides operating with a transverse magnetic (TM) polarized light [27] and slot waveguides operating with a quasi-transverse electric (TE) polarized light [28]. These configurations (strip-TM and slot-TE) have been chosen because they support modes maximizing light-matter interaction outside the dielectric waveguide core. This feature arises from the strong discontinuity of the normal component of the electric field at the interfaces between the silicon core and the surrounding medium. Hence, as shown in Fig. 1, the strip-TM mode (with vertical polarization) is well confined inside the waveguide core with large intensity fields on the top and bottom boundaries. On the other hand, the slot-TE mode (with horizontal polarization) funnels most of the field in the lower index material between two silicon rails. This feature makes the slot an ideal geometry to sense the waveguide surroundings. We will exploit this ability to maximize the interaction between the waveguide mode field and the SWNTs.

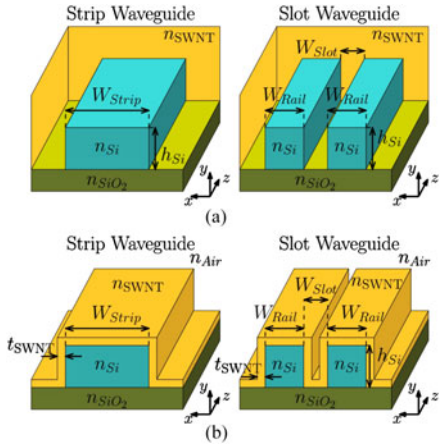

Fig. 2. Schematic views of strip and slot waveguides in: (a) Bulk scenario, corresponding to drop casting SWNTs deposition and (b) surface scenario, corresponding to spin coating SWNTs deposition.

To promote interaction, SWNTs are placed directly on top of the photonic waveguides. To do so, we use two different techniques: drop casting or spin coating. The drop-casting technique yields a highly non-uniform deposition, resulting in different regions with very thick and very thin layers. These regions are arranged along the sample surface following the so-called coffee-ring effect [29]. On the other hand, the spin-coating technique results in a thin layer that maximizes the ratio of deposited SWNTs that can interact with the waveguide evanescent field. However, achieving a good quality and uniform layer with spin-coating technique is challenging, requiring of several repetitions of the process. It is important to note that we process the starting SWNTs solution (composed by metallic and semiconducting SWNTs and impurities) with a polymer-assisted extraction technique [30] to select only semiconducting SWNTs. The mechanism of diameter-selective dispersion of semiconducting SWNTs with polymers was explained recently [31]. This high-selectivity process results in a solution composed of polymer-wrapped semiconducting SWNTs and excess polymer. The drop casting technique yields a relatively thick layer (in the order of a micron) of polymer-wrapped semiconducting SWNTs, while the spin-coating process raises a few nanometer thick layer. To theoretically compare the interaction capability of the strip and slot waveguides we have considered two different simplified scenarios that model these two different deposition techniques. First, we have considered a bulk scenario, depicted in Fig. 2(a), where we assumed that the waveguide is surrounded by a thick (semi-infinite) layer of SWNTs solution, corresponding to drop casting deposition. On the other hand, we have also analyzed a surface scenario described in Fig. 2(b), being the waveguide covered with a thin ($t_{\mathrm{SWNT}} = 10$ nm) SWNTs solution layer that assessed the spin coating deposition technique. The result of the SWNT selection process is a solution of polymer doped with nanotubes. As most of the resulting solution is composed of polymer, we can model the deposited polymer-wrapped SWNTs as a homogenous medium with refractive index of 1.5 similar to that of the polymer [32]. Please note that in these two simplified simulation scenarios we have considered the best deposition case, i.e., waveguides covered with a homogeneous SWNT layer. Hence, we neglected non-uniformities of deposition processes as well as propagation loss due to scattering in the SWNT layer or waveguide side-wall roughness. Nevertheless, this model enables us to fairly compare maximum potential interaction between a SWNT layer and the optical modes of strip and slot waveguides.

As a figure of merit to compare the interaction with SWNTs, we calculated the sensitivity parameter, typically used in photonic biosensors [27]. As performed in previous works [33], we defined bulk and surface sensitivities, respectively, corresponding to the two considered bulk and surface scenarios. Bulk sensitivity in eq. (1), measures the change in the effective index of the guided mode (n_{eff}) upon a change in the refractive index of the cover (n_{SWNT}). Surface sensing (Ss) in eq. (2), relates the change in the index of the waveguide mode (n_{eff}) to an increase in the thickness of the surrounding material (t_{SWNT}),

$$S_B = \frac{\partial n_{\mathrm{eff}}}{\partial n_{\mathrm{SWNT}}} \, [RIU/RIU], \tag{1}$$

$$S_S = \frac{\partial n_{\mathrm{eff}}}{\partial t_{\mathrm{SWNT}}} \, [RIU/nm] \tag{2}$$

where $\partial n_{\mathrm{eff}}$ is the variation in the effective index of the waveguide mode produced either by a modification of the refractive index of the surrounding media ($\partial n_{\mathrm{SWNT}}$ in bulk scenario) or a change in the thickness of the waveguide covering layer ($\partial t_{\mathrm{SWNT}}$ in surface scenario). High sensitivities are directly related to strong interaction with surrounding media [27], [33], which in our case corresponds to the SWNT-rich layer.

Analyzed strip and slot waveguides are implemented on SOI platform with 220 nm thick Si, widely used in state-of-the-art Si photonics. We have calculated the two previously mentioned sensitivities as a function of the main geometrical parameters of the strip and slot waveguides (described in Fig. 2). Strip sensitivity is analyzed as a function of the waveguide width (W_{strip}). For simplicity, in the case of slot waveguides, we have represented slot sensitivity as a function of slot width (W_{slot}) for rail widths of $W_{\mathrm{rail}} = 200$ nm and $W_{\mathrm{rail}} = 250$ nm that maximize sensitivity at the bulk and surface scenarios, respectively. Wavelengths of 1300 and 1550 nm are chosen for this analysis as they correspond to maximum photoluminescence region of HipCo/PFO and Laser/PFO-A [34], respectively. Interestingly, these two wavelength regions are in the center of the O and C bands of the optical fiber, typically used in telecom applications.

For drop casting deposition of SWNTs (bulk scenario in Fig. 3(a) and (b)), slot waveguide sensitivity reaches a plateau around $W_{\mathrm{slot}} = 80$ nm, while strip waveguide sensitivity increases for thinner waveguides. Minimum strip width (and thus maximum sensitivity in this case) is limited by the leakage to the substrate. For spin-coating deposition, slot waveguide sensitivity is inversely proportional to the slot width, being the maximum achievable value limited by the minimum feature size that can be faithfully fabricated. Nevertheless, in all studied cases slot waveguides operating with TE polarized light exhibited larger sensitivity than strip waveguides with TM polarized light. This phenomenon can be qualitatively understood looking at the strip

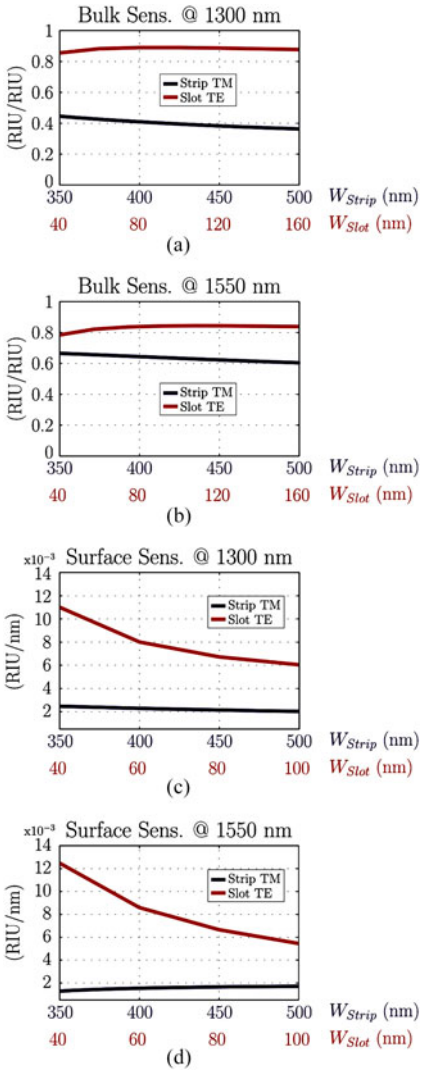

Fig. 3. Calculated sensitivity of strip and slot waveguides for bulk scenario (drop casting SWNT deposition) at (a) 1300 nm and (b) 1550 nm wavelength and surface scenario (spin coating SWNT deposition) at (c) 1300 nm and (d) 1550 nm wavelength.

and slot mode field distribution (Fig. 1). The optical mode in the slot waveguide is much more localized outside silicon (i.e., in the SWNT-rich layer), while for strip waveguides, the mode is more confined inside the silicon core. These results indicate that the slot waveguide can provide larger field overlap with the SWNT-rich layer.

III. Experimental Characterization SWNT Integration on Silicon Photonic Micro-Resonators

Resonant enhancement of SWNT photo-luminescence in a micro-ring resonator is tightly related to the overlap between the SWNTs and the waveguide mode and the waveguide propagation loss [19], [26]. Both, larger SWNTs-waveguide overlap and/or lower propagation losses yield improved resonant enhancement. Hence, to experimentally compare the ability of both waveguides to effectively interact with SWNTs, we have

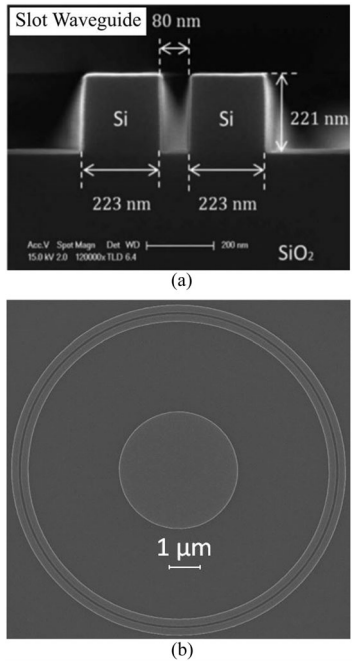

Fig. 4. Scanning electron microscope image of: (a) transversal geometry of slot waveguide and (b) top view of a slot waveguide ring.

fabricated micro-ring resonators using Si strip and slot geometries and we have compared their PL resonance enhancement.

We have fabricated strip and slot ring resonators within the same Si chip, following the same fabrication steps. We have included ring resonators with a radius of $5\ \mu\mathrm{m}$ (to ensure a free-spectral-range discernible with our spectrometer) and different waveguide dimensions. We have set the strip width to 350 nm. For the slot waveguide we changed the slot size between 100 and 200 nm with a fixed rail width of 280 nm. The ring resonators have been fabricated in SOI wafers with 220 nm thick silicon film and $2\ \mu\mathrm{m}$ of buried silica layer. Electron beam lithography (Nanobeam NB-4 system, 80 kV) has been used to define the micro-rings. A dry etching process with an inductively coupled plasma etcher (SF6 gas) transferred the patterns in the top Si layer. Following, a dry oxidation process was adopted at 1000 °C for 30 min to form a $\sim 10\ \mathrm{nm}$ thick silica surrounding silicon rails. The de-oxidation was performed by dipping the sample for 7 s in a 3% HF acid solution at 25 °C in order to smooth the sidewall roughness of the waveguide. The technology developed here was optimized to reduce the optical propagation loss of the waveguides [35]. Fig. 4 shows scanning electron microscope (SEM) images of transversal geometry of slot waveguide and a top view of a slot waveguide ring. For fabrication convenience all the structures have a Si microdisk of $2\ \mu\mathrm{m}$ concentric with the microring. We have linearly characterized strip and slot ring resonators of $5\ \mu\mathrm{m}$ radius connected to bus waveguides. We have estimated intrinsic quality factors in the order of a few thousands for slot resonators and few tens of thousands for strip resonators. This indicates a larger propagation loss in slot compared with strip waveguides.

We deposited the same SWNT solution simultaneously over the strip and slot rings. We spin coated the SWNTs at 1000 rpm

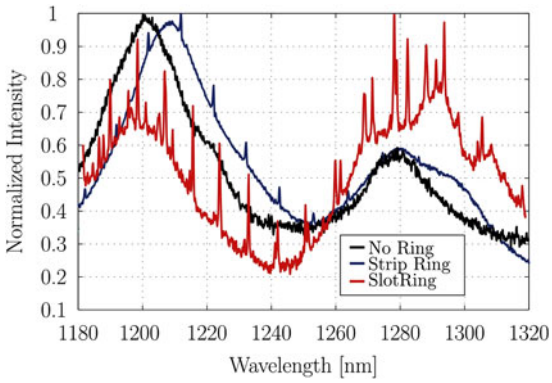

Fig. 5. PL intensity as a function of the wavelength when: Excitation beam is focused onto un-patterned Si region (blackline) strip micro-ring (blue line) and slot micro-ring (red line). The pump wavelength was 735 nm.

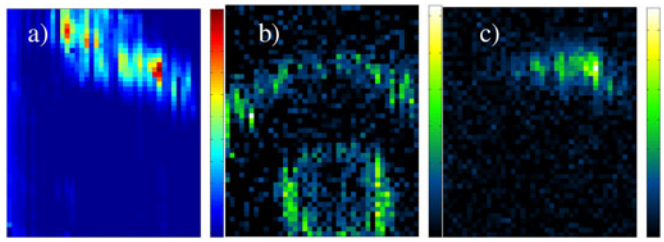

Fig. 6. Spatial maps of for a Si strip microring of 5 μm with an inner microdisk of 2 μm. The pump wavelength was 735 nm and the spatial resolution is of the order of 1 μm and the maps are 9 μm $\times$ 10 μm in size. Panel (a) spatial map of the integrated SWNT PL signal from 1290 to 1310 nm. Panel (b) spatial map of the enhanced Si PL at 1150 nm. Panel (c) spatial map of the enhanced SWNT PL from 1290 to 1310 nm.

during 60 s, finishing by thermal annealing of 15 min at 180 °C. This process was then repeated several times to improve the layer uniformity and hence the average concentration of carbon nanotubes over the sample.

We used a Titane Sapphire (Ti:Sa) laser, pumped by a continuous wave solid state laser, as light source. We excite the deposited SWNTs at a wavelength 735 nm, in the middle of the S_{22} transition bands of (8,6) and (8,7) SWNTs with 1 mW (measured just before of microscope). The Ti:Sa excitation beam passes through a low –pass wavelength filter (to remove higher order harmonics of the laser) and is driven towards the microscope that performs a double functionality. First, it is used to focus the pump within the region of interest in the Si sample, using a 50x microscope objective. Then, the microscope objective also collects the SWNT emission, with the same objective, directing it to a high-pass wavelength filter (to remove the excitation beam) before entering the spectrometer. PL is recorded with a 320 mm spectrometer with a 950 lines/mm grating, using a nitrogen–cooled 512-pixel linear InGaAs array. PL characterization is performed at room temperature.

Fig. 5 represents measured light emission under the same experimental conditions from SWNTs when we pumped on different positions along the same Si sample comprising strip and slot micro-ring resonators. In black line we represent the PL when we focus the pump outside of rings. We can observe two wide-band emission peaks around 1200 and 1280 nm wavelengths that correspond to the emission from nanotubes with chiralities of (8,6) and (8,7), in good agreement with the results of the polymer-assisted selection technique [30]. However, other wide-band emission peaks can be observed, for instance around 1280 nm wavelength in the slot ring spectra, associated to the emission of other SWNTs with different chiralities that are still present in the processed solution. In blue line, we plot the collected PL when we focused the pump on top of the strip micro-ring resonator (of 350 nm width) that showed the largest resonance enhancement. In this case, narrow-band PL enhancement peaks appear superimposed onto the SWNT's emission. These peaks are induced by resonance inside the micro-ring [19]. Finally, in red line, we represent the measured PL when we focused the pump onto the slot micro-ring resonator under the same measurement conditions. Please note that both, TE and TM, modes inside the ring resonators can be excited during optical pumping, resulting in two sets of resonance peaks. Interestingly, despite their larger propagation loss, slot ring resonators exhibit better resonant-enhancement peaks. This indicates that the improved interaction between SWNTs and optical waveguide mode overcomes the additional loss.

In order to demonstrate the coupling of the SWNTs with the photonic modes, we report in Fig. 6 three different PL spatial maps for a Si strip microring of 5 μm. The pump wavelength was 735 nm and the spatial resolution is of the order of 1 μm. We measured the PL spectra with a spatial scan in a region of 9 μm $\times$ 10 μm at step of 200 nm. Fig. 6 reports the integrated SWNT PL emission intensity [panel (a)] and the intensity of the photonic resonance peaks over the Si PL emission [panel (b)] and over the SWNT PL emission at 1300 nm [panel (c)]. The contributions of the enhanced PL reported in panels (b) and (c) have been obtained by fitting the resonance peaks by Lorentzians lineshapes. Bright spots in the map in panel a) correspond to the regions where the SWNTs are deposited, showing a non-uniform pattern typical from spin-coating deposition. Therefore from the maps in panels (a)-(c) we clearly show that the enhanced SWNT PL emission is limited to the region where the deposited nanotubes are overlapped to the Si ring. Eventually, this proves the coupling between SWNTs and the photonic modes of the silicon microring.

To quantitatively compare strip and slot microrings, we define here the PL resonance enhancement factor (Γ) as the ratio between the peak PL at micro-ring resonance (PL_{Peak}) and the background PL from SWNT emission (PL_{SWNT}):

$$\Gamma = \frac{PL_{\mathrm{Peak}}}{PL_{\mathrm{SWNT}}}. \tag{3}$$

Slot micro-ring resonators exhibit a resonance enhancement factor of $\Gamma \sim 1.8$ clearly larger than the strip micro-rings'ones $(\Gamma \sim 1.1)$, proving an improved performance of slotted structures for the integration of SWNTs on silicon. This result is in good agreement with our theoretical analysis, and can be explained by the fact that the light interaction in slot waveguides is stronger than in strip waveguides, overcoming the typically larger propagation loss.

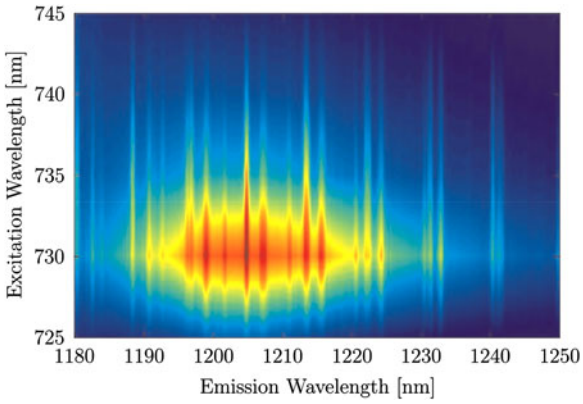

Fig. 7. PL intensity of Si slot micro-ring resonator with $5\,\mu\mathrm{m}$ radius and 170 nm slot width, as a function of the excitation and emission wavelengths.

Finally, Fig. 7 shows wavelength PL response of a typical fabricated slot micro-ring resonator as a function of the excitation wavelength. It is possible to distinguish the micro-ring resonance enhancement of the PL (sharp peaks along the emission wavelength) as well as the effect of exciting the SWNT in and out of their absorption band, around 730 nm for (8,6) chirality SWNTs with emission around 1200 nm.

IV. Conclusions

SWNTs are a material studied in microelectronics able to emit and absorb near-infrared light at room temperature. These characteristics make them a very promising material for the implementation of sources and photodetectors integrated onto Si photonic devices for on-chip communications/telecom applications and optical bio-sensing. This way, SWNT exhibit various key fundamental properties that enable the development a complete library of active building blocks for the Si photonic technology, including sources, detectors and modulators. All these active devices could, in principle, be monolithically integrated with Si photonics in a single process, alleviating the issues of current 3-D or hybrid integration schemes. One key challenge towards the development of such SWNT-based photonic library is to maximize the interaction of SWNTs and Si photonic waveguides, i.e., optimizing waveguide geometry to maximize mode field overlap with SWNT while maintaining appropriate propagation loss. In this work we proposed, to use Si slot waveguides to improve interaction with SWNTs, compared with previously used strip waveguides. We theoretically analyzed and experimentally compared the ability of photonic Si strip and slot waveguides to interact with solution-processed semiconducting SWNTs deposited onto Si photonic chip. We have characterized the photoluminescence enhancement provided by Si strip and slot micro-rings fabricated on SOI platform. Slot micro-ring resonators showed a $\sim 60\%$ larger resonance enhancement in comparison with strip waveguide micro-resonators. These results open a new path towards the effective integration of SWNTs into Si photonic devices.

References

[1] H. Liu, C. F. Lam, and C. Johnson, "Scaling optical interconnects in datacenter networks," in *Proc. 18th IEEE Symp. High Perform. Interconnects*, 2010, pp. 113–116.
[2] Y. A. Vlasov, "Silicon CMOS-integrated nano-photonics for computer and data communications beyond 100G," *IEEE Commun. Mag.*, vol. 50, no. 2, pp. s67–s72, Feb. 2012.
[3] C. Gunn, "CMOS photonics for high-speed interconnects," *IEEE Micro.*, vol. 26, no. 2, pp. 58–66, Mar./Apr. 2006.
[4] L. Wosinski and Z. Wang, "Integrated silicon nanophotonics: A solution for computerinterconnects," in *Proc. IEEE Int. Conf. Transparent Opt. Netw.*, 2011, pp. 1–4.
[5] M.-C. Estévez, M. Álvarez, and L. M. Lechuga, "Integrated optical devices forlab-on-a-chip biosensing applications," *Laser & Photon. Rev.*, vol. 6, no. 4, pp. 463–487, 2012.
[6] R. Soref, "Mid-infrared photonics in silicon and germanium," *Nature Photonics*, vol. 6, no. 4, pp. 463–487, 2012.
[7] L. Vivien and L. Pavesi, *Handbook of Silicon Photonics*. Boca Raton, FL, USA: CRC Press, 2013.
[8] S. Assefa, W. M. Green, A. Rylyakov, C. Schow, F. Horst, and Y. Vlasov, "CMOSintegrated nanophotonics: Enabling technology for exascale computing systems," in *Proc.OSA Optical Fiber Commun. Conf.*, 2011, pp. 1–4.
[9] M. Salib, M. Morse, and M. Paniccia, "Opportunities and integration challengesfor CMOS-compatible silicon photonic and optoelectronic devices," in *Proc. IEEE Int. Conf. Group IV Photonics*, 2004, pp. 1–6.
[10] X. Zheng *et al.*, "Ultralow power 80 Gb/s arrayed CMOS silicon photonic transceivers for WDM optical links," *J. Lightw. Technol.*, vol. 30, no. 4, pp. 641–650, Feb. 2012.
[11] B. Ben Bakir, A. Descos, N. Olivier, D. Bordel, P. Grosse, E. Augendre, L. Fulbert, and J. M. Fedeli, "Electrically driven hybrid Si/III-V Fabry-Pérot lasers based on adiabatic mode transformers," *Opt. Express*, vol. 19, no. 11, pp. 10317–10325, 2011.
[12] L. Virot, P. Crozat, J-M. Fédéli, J-M. Hartmann, D. Marris-Morini, E. Cassan, F. Bœuf, and L. Vivien, "Germanium avalanche receiver for low power interconnects," *Nature Commun.*, vol. 5, pp. 4957-1–4957-6, 2014.
[13] D. Marris-Morini *et al.* "Recent progress in high-speed silicon-based optical modulators," *Proc. IEEE*, vol. 97, no. 7, pp. 1199–1215, Jul. 2009.
[14] ITRS Roadmap, "International technology roadmap for semiconductors," Executive Summary. Semiconductor Industry Association, 2009.
[15] Q. Cao, S-J. Han, J. Tersoff, A. Franklin, Y. Zhu, Z. Zhen, G. Tulevski, J. Tang, and W. Haensch, "End-bonded contacts for carbon nanotube transistors with low, size-independent resistance," *Science*, vol. 350, no. 6256, pp. 68–72, 2015.
[16] E. Gaufrès, N. Izard, A. Noury, X. L. Roux, G. Rasigade, A. Beck, and L. Vivien, "Light emission in silicon from carbon nanotubes," *ACS Nano*, vol. 6, no. 5, pp. 3813–3819, 2012.
[17] M. Yoshida, Y. Kumamoto, A. Ishii, A. Yokoyama, and Y. Kato, "Stark effect of excitons in individual air-suspended carbon nanotubes," *Appl. Phys. Lett.*, vol. 105, no. 16, 2014, Art. no. 161104.
[18] V. Margulis, E. A. Gaiduk and E. N. Zhidkin, "Quadratic electro-optic effects in semiconductor carbon nanotubes," *Phys. Lett. A*, vol. 258, no. 4, pp. 394–400, 1999.
[19] A. Noury, X. Le Roux, L. Vivien, and N. Izard, "Controlling carbon nanotube photoluminescence using silicon microring resonators," *Nanotechnology*, vol. 25, no. 11, 2014, Art. no. 215201.
[20] E. Gaufrès, N. Izard, X. Le Roux, D. Marris-Morini, S. Kazaoui, E. Cassan, and L. Vivien, "Optical gain in carbon nanotubes," *Appl. Phys. Lett.*, vol. 96, no. 23, 2010, Art. no. 231105.
[21] R. Watahiki, T. Shimada, P. Zhao, S. Chiashi, S. Iwamoto, Y. Arakawa, S. Maruyama, and Y. K. Kato, "Enhancement of carbon nanotube photoluminescence by photonic crystal nanocavities," *Appl. Phys. Lett.*, vol. 101, no. 14, 2012, Art. no. 141124.
[22] H. Sumikura, E. Kuramochi, H. Taniyama, and M. Notomi, "Cavity-enhanced Raman scattering of single-walled carbon nanotubes," *Appl. Phys. Lett.*, vol. 102, no. 23, 2013, Art. no. 231110.
[23] S. Imamura, R. Watahiki, R. Miura, T. Shimada, and Y. K. Kato, "Optical control of individual carbon nanotube light emitters by spectral double resonance in silicon microdisk resonators," *Appl. Phys. Lett.*, vol. 102, no. 16, 2013, Art. no. 161102.
[24] R. Miura, S. Imamura, R. Ohta, A. Ishii, X. Liu, T. Shimada, S. Iwamoto, Y. Arakawa, and Y. Kato, "Ultralow mode-volume photonic crystal

nanobeam cavities for high-efficiency coupling to individual carbon nanotube emitters," *Nature Commun.*, vol. 5, pp. 5580-1–5580-5, 2014.

[25] E. Gaufrès, N. Izard, X. Le Roux, S. Kazaoui, D. Marris-Morini, E. Cassan, and L. Vivien, "Optical microcavity with semiconducting single-wall carbon nanotubes," *Opt. Express*, vol. 18, no. 6, pp. 5740–5745, 2010.

[26] A. Noury, X. Le Roux, L. Vivien, and N. Izard, "Enhanced light emission from carbon nanotubes integrated in silicon micro-resonator," *Nanotechnology*, vol. 26, no. 34, 2015, Art. no. 345201.

[27] A. Densmore *et al.* "A silicon-on-insulator photonic wire based evanescent field sensor," *IEEE Photon. Technol. Lett.*, vol. 18, no. 23, pp. 2520–2522, Dec. 2006.

[28] V. R. Almeida, Q. Xu, C. A. Barrios, and M. Lipson, "Guiding and confining light in void nanostructure," *Opt. Lett.*, vol. 29, no. 11, pp. 1209–1211, 2004.

[29] A. Shimoni, S. Azoubel and S. Magdassi, "Inkjet printing of flexible high-performance carbon nanotube transparent conductive films by coffee ring effect," *Nanoscale*, vol. 6, pp. 11084–11089, 2014.

[30] N. Izard, S. Kazaoui, K. Hata, T. Okazaki, T. Saito, S. Iijima, and N. Minami, "Semiconductor-enriched single wall carbon nanotube networks applied to field effect transistors," *Appl. Phys. Lett.*, vol. 92, no. 24, 2008, Art. no. 243112.

[31] H. Yang, V. Bezugly, J. Kunstmann, A. Filoramo, and G. Cuniberti, "Diameter-selective dispersion of carbon nanotubes via polymers: a competition between adsorption and bundling," *ACS Nano*, vol. 9, 2015, Art. no. 9012.

[32] M. Campoy-Quiles, P. G. Etchegoin, and D. D. C Bradley, "Exploring the potential of ellipsometry for the characterisation of electronic, optical, morphologic and thermodynamic properties of polyfluorene thin films," *Synthetic Metals*, vol. 155, no. 2, pp. 279–282, 2005.

[33] J. G. Wangüemert-Pérez, P. Cheben, A. Ortega-Moñux, C. Alonso-Ramos, D. Pérez-Galacho, R. Halir, I. Molina-Fernández, D.-X. Xu, and J.H. Schmid, "Evanescent field waveguide sensing with subwavelength grating structures in silicon-on-insulator," *Opt. Lett.*, vol. 39, no. 15, pp. 4442–4445, 2014.

[34] A. Nish, J. Y. Hwang, J. Doig, and R. J. Nicholas,"Highly selective dispersion of single-walled carbon nanotubes using aromatic polymers," *Nature Nanotechnol.*, vol. 2, no. 10, pp. 640–646, 2007.

[35] W. Zhang, S. F. Serna Otálvaro, X. Le Roux, L. Vivien, and E. Cassan, "Design, fabrication and optimization of silicon slot photonic ring resonators," in *Proc. OSA Asia Commun. Photonics Conf.*, 2014, pp. AF1B–2.

Authors' biographies not available at the time of publication.